Mon. Not. R. Astron. Soc. **000**, 000–000 (0000) Printed 1 February 2008 (MN LaTeX style file v2.2)

arXiv:astro-ph/0111559v2 15 Jan 2002

A submillimetre difference between radio galaxies and radio quasars: evidence for quasar-heated dust and synchronized submillimetre and radio source activity

Chris J. Willott[1]*, Steve Rawlings[1], Elese N. Archibald[2] & James S. Dunlop[3]
[1] *Astrophysics, Department of Physics, Keble Road, Oxford, OX1 3RH, U.K.*
[2] *Joint Astronomy Centre, 660 N. Aʻohōkū Place, University Park, Hilo, Hawaii, 9620, USA*
[3] *Institute for Astronomy, University of Edinburgh, Blackford Hill, Edinburgh, EH9 3HJ, UK*

1 February 2008

ABSTRACT

We present submillimetre photometry of 11 3CR and 6CE radio quasars of similar 151-MHz radio luminosity and redshifts to the radio galaxies studied at $1.3 < z < 2$ by Archibald et al. (2001). We detect all bar one quasar at 850 μm, and five quasars are confirmed as dusty hyperluminous objects by detections at shorter wavelengths. Our observations reveal a clear difference between the submillimetre luminosity distributions of the radio quasars and a matched sample of radio galaxies: the quasars are ~ 5-times brighter than the radio galaxies and $\geqslant 2$-times brighter accounting for possible synchrotron contamination. This difference is in quantitative agreement with a receding-torus unified scheme for radio sources in which the torus opening angle depends on quasar optical luminosity, provided that there is a close relationship between the optical and submillimetre luminosities. The implication is that quasar-heated dust dominates the submillimetre emission for powerful radio quasars at $z \sim 1.5$. We find a significant anti-correlation between submillimetre/far-infrared luminosity $L_{\rm FIR}$ and radio source age in the sense that hyperluminous quasars tend to be associated with young ($< 10^7$ yr) sources. This suggests that the processes controlling $L_{\rm FIR}$ are synchronized with the jet-triggering event and that $L_{\rm FIR}$ declines on a $\sim 10^7$ yr timescale. There is evidence for a small amount of obscuration in the hyperluminous quasars from reddening and associated or broad absorption lines. We speculate that shortly after jet triggering, dust is more widely distributed than at later times and is heated by the quasar nucleus and/or a short-lived synchronized starburst. Any such starburst would form only a few per cent of the total stellar mass in agreement with the evidence for dominant old stellar populations in $z \sim 1.5$ radio galaxies. In contrast, high-redshift ($z > 3$) radio galaxies with similar submillimetre luminosities could have longer star-formation timescales due to the greater availability of gas and could be forming the bulk of their stellar populations.

Key words: galaxies: active – galaxies: evolution – quasars: individual: 3C 268.4, 3C 298, 3C 318, 6C 1045+3513

1 INTRODUCTION

Submillimetre observations provide an excellent method of detecting dusty star-forming galaxies at high redshifts: UV radiation from hot stars is absorbed by dust, re-radiated in the far-infrared and redshifted into the submillimetre. The steep submillimetre spectral index leads to large k-corrections which, at high redshifts, compensates for increasing cosmological dimming so that an object with a given submillimetre luminosity has a similar observed flux-density at $z = 1$ to a similarly-luminous one at $z = 5$ (Blain & Longair 1993).

Powerful radio sources can be easily identified out to high redshifts and are thought to be associated with massive elliptical galaxies, or their progenitors. The existence of this close association is well known at low-to-intermediate

---

* Email: cjw@astro.ox.ac.uk

redshifts (e.g. Owen & Laing 1989) and it is likely to be maintained to higher redshifts by scaling relations between radio luminosity, accretion luminosity, black hole mass and (dark matter) halo mass (e.g. Rawlings & Saunders 1991; Magorrian et al. 1998). At low-redshifts, radio galaxies appear to be kinematically-relaxed massive ellipticals (McLure et al. 1999; Dunlop et al. 2001; Bettoni et al. 2001) with old stellar populations (Nolan et al. 2001). These facts, together with the small scatter in the near-infrared Hubble diagram to $z \approx 3$ (Jarvis et al. 2001a), suggest that most of the star formation in powerful radio galaxies occurred at early cosmic epochs.

In the first large study of the submillimetre emission of high-redshift radio galaxies, Archibald et al. (2001; hereafter A01) made sensitive (850 μm sensitivity ≈ 1 mJy rms) submillimetre observations of 47 radio galaxies with the SCUBA array on the JCMT. Their sample covered the redshift range $1 < z < 4.5$ and they detected dust emission in 14 objects. The main result of their study was a clear difference between the detection rate at $z < 2.5$ of 15% and the detection rate at $z > 2.5$ of 75%. This indicates that the submillimetre luminosity of radio galaxies increases systematically with redshift, suggesting that the bulk of star formation in radio galaxies, and by inference in all massive galaxies, occurred at epochs corresponding to high redshifts.

Unified schemes for radio galaxies and radio quasars[1] propose they are the same objects viewed along different lines-of-sight, such that in radio galaxies the nuclear regions are obscured by a dusty torus or warped disc (Scheuer 1987; Barthel 1989). Such theories have proved remarkably successful (see Antonucci 1993 for a review), at least at high radio luminosities (Willott et al. 2000a). For objects at redshifts $z \approx 1.5$, the observed 850 μm radiation was emitted at a rest-frame wavelength of ≈ 300 μm. At these wavelengths, dust is expected to be optically thin and its thermal emission isotropic (e.g. Granato & Danese 1994; Efstathiou & Rowan-Robinson 1995). Therefore, according to the simplest type of radio-loud AGN unification scheme, the submillimetre properties of radio galaxies and radio quasars, matched in terms of low-frequency radio luminosity and redshift, should be similar. In more realistic unified schemes, however, they may not be expected to be identical. Rawlings & Saunders (1991) and Simpson (1998) have argued that samples of radio galaxies and radio quasars, matched in one orientation-independent quantity (i.e. low-frequency radio luminosity), are expected to have different distributions in a second orientation-independent quantity (i.e. [O III] emission line luminosity) if the two quantities are linked by a scaling relation with intrinsic scatter. The first motivation behind the work described in this paper was to explore unified schemes further by looking for significant differences between the submillimetre properties of radio galaxies and radio quasars matched in 151-MHz luminosity and redshift.

The second motivation behind this paper was to explore further the suggestion of Blundell & Rawlings (1999) that some part of the evolution in the submillimetre properties of radio galaxies with redshift is a selection effect linked to the inevitable youth of the highest-redshift radio sources from flux-limited samples. A01 have already considered this suggestion, arguing that it is not a primary driver of the observed redshift dependencies. However, with a small dynamic range in source age, and somewhat uncertain selection effects, the high-redshift sample of Archibald et al. is not ideally suited to a test of the idea that submillimetre properties might be correlated with the time since the jet-triggering event.

At $z \sim 1.5$ A01 have already obtained submillimetre data on an unbiased sample of 3CRR and 6CE galaxies, and we aimed to complement these with new observations of a matched sample of radio quasars. In Section 2 we describe the observations and results. In Section 3 we consider the likely contribution to the measured submillimetre fluxes from an extension of the radio synchrotron spectrum. In Section 4 we consider explanations for our results. We present our conclusions in Section 5. The convention for all spectral indices α is that flux-density $S_\nu \propto \nu^{-\alpha}$. We assume throughout that $H_0 = 70$ km s^{-1}Mpc^{-1}, $\Omega_{\rm M} = 0.3$ and $\Omega_\Lambda = 0.7$.

2 OBSERVATIONS

We have defined a sample of radio quasars in the redshift range $1.37 < z < 2.0$ selected from two complete radio samples (3CRR – Laing, Riley & Longair 1983; 6CE – Rawlings, Eales & Lacy 2001) to compare with the radio galaxies from the same samples in the same redshift range in the study of A01. Due to scheduling reasons only 3CRR quasars within the Right Ascension range $04^{\rm h} <$ RA $< 22^{\rm h}$ are included in our sample. These were supplemented with two quasars from the revised 3C catalogue (3CR – Spinrad et al. 1985). These two quasars, 3C 298 and 3C 280.1, are not included in the 3CRR sample due to reasons of low declination and radio flux-density just below the 3CRR limit, respectively. They are the only high galactic latitude quasars in the target redshift range in the 3CR sample which are not included in the 3CRR sample. The total sample consists of 11 quasars and the comparison sample extracted from A01 contains 12 radio galaxies (Table 1).

The sample of radio quasars was observed in photometry mode with the SCUBA bolometer array at the JCMT in March, April, October 1999, November 2000, February and April 2001. Observations were made simultaneously at 850 μm and 450 μm and the sensitivities reached at 850 μm are ∼ 1 mJy rms. The atmospheric zenith opacity at 850 μm ranged from 0.16 to 0.52 with a median of 0.22. The data were reduced using the SURF package, following the same method as in A01 for consistency. The resulting flux-densities are given in Table 1 along with the data for the matched radio galaxy sample. Ten out of eleven radio quasars were detected at 850 μm at $> 2\sigma$ significance (eight at $> 3\sigma$), compared with only four $> 2\sigma$ detections out of the twelve radio galaxies. At the shorter wavelength of 450 μm, three quasars have $> 2\sigma$ detections, compared to none

---

[1] We will use the term 'radio quasars' to refer to lobe-dominated steep-spectrum radio sources associated with quasar nuclei. These are the dominant population of radio-loud quasars in low-frequency-selected samples such as 3CRR and 6CE, whereas compact flat-spectrum quasars dominate in high-frequency-selected samples. Flat-spectrum quasars often have high submillimetre fluxes simply by virtue of a continuation of their synchrotron spectra from radio to shorter wavelengths.

Name	Class	Redshift z	$\log L_{151}$ W/Hz/sr	$S_{\rm core}$ mJy	$\log L_{\rm [O\,III]}$ W	D kpc	S_{850} (mJy)	S_{450} (mJy)	S_{850} 2σ limit	S_{450} 2σ limit
3C 181	Q	1.382	28.11	6.0	37.37	48.0	$\mathbf{5.27} \pm 1.06$	-0.8 ± 7.5	–	15
3C 191	Q	1.952	28.52	38.3	37.21	41.1	$\mathbf{6.39} \pm 1.06$	$\mathbf{28.9} \pm 8.1$	–	–
3C 205	Q	1.534	28.19	24.6	37.00	152.4	$\mathbf{2.36} \pm 1.10$	11.6 ± 7.9	–	27
3C 268.4	Q	1.400	27.97	42.9	37.25	91.9	$\mathbf{5.13} \pm 1.18$	9.9 ± 12.5	–	35
3C 270.1	Q	1.519	28.24	60.0	36.51	101.6	$\mathbf{7.42} \pm 1.17$	15.4 ± 11.5	–	38
3C 280.1	Q	1.659	28.36	36.0	36.72	39.8	$\mathbf{5.10} \pm 1.74$	0.4 ± 23.8	–	48
3C 298	Q	1.439	28.57	515	37.26	12.7	$\mathbf{21.13} \pm 2.06$	-8.0 ± 23.7	–	47
3C 318	Q	1.574	28.11	22.0	37.18	6.8	$\mathbf{7.78} \pm 1.00$	$\mathbf{21.6} \pm 10.6$	–	–
3C 432	Q	1.785	28.31	7.5	36.68	109.8	$\mathbf{7.93} \pm 1.70$	2.91 ± 20.9	–	45
6C 0955+3844	Q	1.405	27.45	4.3	36.58	181.3	-0.01 ± 1.11	8.9 ± 7.8	2.22	25
6C 1045+3513	Q	1.594	27.22	10.0	35.94	1.7	$\mathbf{9.18} \pm 1.10$	$\mathbf{21.3} \pm 6.8$	–	–
4C 13.66	G	1.450	28.09	0.8	36.63	50.7	$\mathbf{3.53} \pm 0.96$	-16.2 ± 18.2	–	36
3C 239	G	1.781	28.42	0.5	36.38	94.6	0.83 ± 1.00	-2.1 ± 18.3	2.83	37
3C 241	G	1.617	28.11	5.0	36.75	7.7	1.81 ± 0.94	14.8 ± 12.6	3.69	40
3C 294	G	1.786	28.39	0.5	36.97	126.7	0.19 ± 0.78	5.4 ± 13.4	1.75	32
3C 322	G	1.681	28.21	2.2	35.97	279.4	-0.05 ± 1.06	-37.5 ± 16.0	2.12	32
3C 437	G	1.480	28.11	0.1	36.38	291.0	-1.18 ± 0.98	2.9 ± 17.3	1.96	37
3C 470	G	1.653	28.15	2.0	35.93	203.2	$\mathbf{5.64} \pm 1.08$	57.8 ± 32.9	–	124
6C 0820+3642	G	1.860	27.55	1.0	36.00	193.8	$\mathbf{2.07} \pm 0.96$	13.6 ± 18.0	–	50
6C 0901+3551	G	1.904	27.46	0.5	36.12	21.9	-1.83 ± 1.15	-19.3 ± 8.2	2.30	16
6C 0905+3955	G	1.882	27.71	1.1	35.76	934.5	$\mathbf{3.62} \pm 0.89$	31.2 ± 16.2	–	64
6C 0919+3806	G	1.650	27.53	6.0	34.96	88.1	-0.88 ± 1.05	10.5 ± 10.1	2.10	31
6C 1204+3708	G	1.779	27.61	1.0	36.45	435.2	0.16 ± 1.25	45.1 ± 26.6	2.66	98

Table 1. Submillimetre observations and basic data for the sample of radio quasars (class 'Q') and radio galaxies ('G') in the redshift range $1.37 < z < 2.0$ described in Sec. 2. Detections at the $\geqslant 2\sigma$ level are given in bold type. Submillimetre flux-densities of the radio galaxies are from A01. No corrections have been made for possible contributions of synchrotron emission to the submillimetre fluxes. Radio core fluxes are quoted at 5 GHz (observed-frame) in most cases. Radio data for the radio galaxies and quasars are from the references listed in A01 and Blundell et al. (in prep.) respectively. Data for the [O III] emission line luminosities have been taken from Jackson & Rawlings (1997) for 3CR sources and Rawlings et al. (2001) for 6C sources, apart from these exceptions: 3C 241 – Hirst, Jackson & Rawlings (2002); 3C 270.1 and 6C 0955+3844 – Willott et al. (in prep.); 3C 298 – Espey et al. (1989); 3C 318 – Willott et al. (2000b); 6C 1045+3513 (this paper). For some sources, [O III] has not been observed and a different narrow line flux is used and the [O III] flux estimated from the line ratios in McCarthy (1993). These sources are 3C 298 ([O II]); 6C 0820+3642 (Lyα); 6C 0901+3551(Lyα); 6C 0905+3955 (Lyα); 6C 0919+3806 (C II]); 6C 1045+3513 ([Ne V]); 6C 1204+3708 (Lyα). For the quasar 3C 432, no narrow line data have been published and the [O III] flux has been estimated assuming a rest-frame equivalent width of 30 Å (e.g. Miller et al. 1992).

of the radio galaxies (although the quasar observations are generally more sensitive at 450 μm than those of the radio galaxies due to the introduction of new filters in October 1999). The mean quasar S_{850} is 6.3 ± 1.0 mJy and the mean radio galaxy S_{850} is 1.2 ± 0.6 mJy. Therefore the quasars are brighter than the radio galaxies in the submillimetre by a factor of 5.

Relating the observed submillimetre flux-density to a submillimetre/far-infrared luminosity is not a trivial matter, given the poor constraints on the shape of the dust spectra for most sources which have only been detected at one or two wavelengths. Therefore, we adopt a template dust spectrum as has been determined from observations of a sample of similarly luminous (submillimetre/far-infrared luminosities $L_{\rm FIR} \sim 10^{13} L_{\odot}$) objects by Priddey & McMahon (2001). This template consists of isothermal optically-thin dust with temperature $T = 41$ K and emissivity index $\beta = 1.95$. For our adopted cosmological model and dust template, the observed 850μm flux-density S_{850} of a source with a given $L_{\rm FIR}$ does not change appreciably over the redshift range $z = 1$ to $z = 5$. The conversion between $L_{\rm FIR}$ and S_{850} for our adopted dust spectrum is $L_{\rm FIR} \approx 2 \times 10^{12} (S_{850}/{\rm mJy}) L_{\odot}$. However, for higher dust temperatures or multi-temperature models (which are required to fit the infra-red SEDs of most luminous AGN – e.g. Rowan-Robinson 2000), $L_{\rm FIR}$ could be up to an order of magnitude greater than this, so these values of $L_{\rm FIR}$ should be treated as lower limits. Therefore the radio quasars we have detected with SCUBA have lower limits on their far-infrared luminosities in the range 4×10^{12} to $2 \times 10^{13} L_{\odot}$. It is likely that many of them would be classified as hyperluminous infrared sources ($L_{\rm FIR} \geqslant 10^{13} L_{\odot}$) if their far- and mid-infrared fluxes were measured. Throughout most of this paper we will use the observed submillimetre flux-density in preference to the far-infrared luminosity and thereby avoid uncertainty in $L_{\rm FIR}$ due to the unknown dust spectral shape.

Five of the radio quasars are also detected at wavelengths shorter than 850μm. 3C 191, 3C 318 and 6C 1045+3513 are detected at 450μm with SCUBA and 3C 268.4, 3C 298 and 3C 318 are detected in the far-infrared by ISO and/or IRAS. These objects are discussed in further detail here.

2.1 Notes on objects detected at $100 - 450$μm

3C 191

The submillimetre spectral index of 3C 191 determined from the 850μm and 450μm fluxes is -2.4 ± 0.6, consistent within 2σ with the value of -3.2, expected for our assumed dust template. We find that $L_{\rm FIR} > 1.2 \times 10^{13} L_{\odot}$. The op-

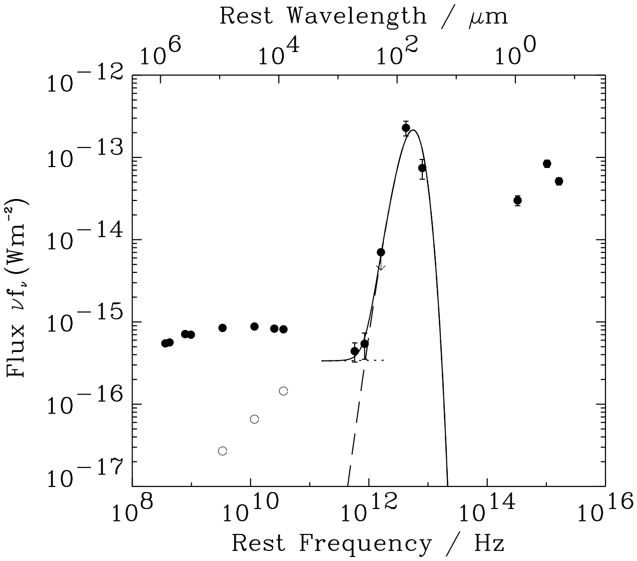

Figure 1. Rest-frame SED from radio to optical of the hyperluminous IR quasar 3C 268.4. For observations which separate the core emission from that of the extended radio components, the core flux is shown as an open circle. The dotted line is a $\alpha = 1$ core spectrum which dominates the millimetre flux. The dashed curve is the best fit thermal dust spectrum ($T = 48$ K, $\beta = 2.5$, optically-thin at $\lambda > 50\mu$m). The solid curve shows this added to the synchrotron core spectrum.

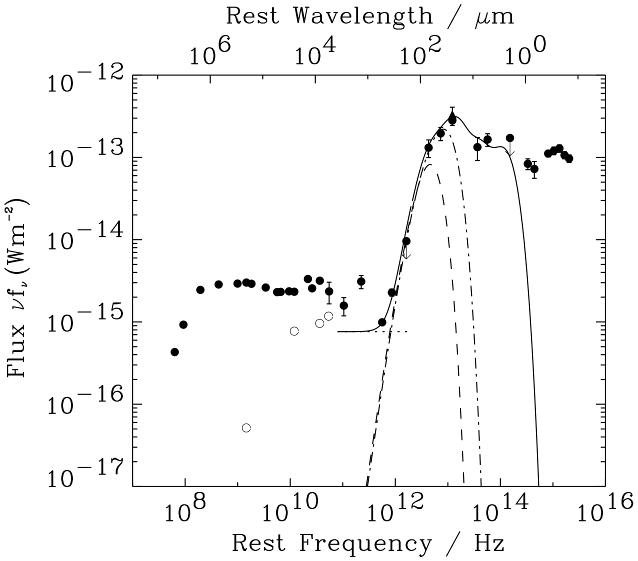

Figure 2. Rest-frame SED of the hyperluminous IR quasar 3C 298 – symbols as for Fig. 1. The dotted line is a $\alpha = 1$ core spectrum which dominates the millimetre flux. The solid curve shows this added to the thermal IR spectrum which is modelled as a combination of greybodies of temperatures ranging from 50 K (this component is shown by a dashed line) to 1300 K. The dot–dashed line shows that the submillimetre/far-infrared data points could equally well be fitted by a T=100 K dust spectrum.

tical spectral slope is $\alpha_{\rm opt} = 0.7$ (Barthel, Tytler & Thomson 1990), quite similar to the typical radio quasar value of $\alpha_{\rm opt} = 0.5$ (Brotherton et al. 2001). This indicates that there is little reddening of the quasar light along our line-of-sight. However, 3C 191 has very strong associated absorption lines with a C IV absorption equivalent width of 6.1 Å (Anderson et al. 1987). Hamann et al. (2001) studied these absorption systems with high-resolution spectroscopy and determined the distance of the absorbers from the nucleus to be ≈ 30 kpc with a corresponding characteristic flow time of 3×10^7 years. The distances of the radio hotspots from the nucleus are of a similar size-scale (projected linear size=41 kpc), corresponding to an approximate age of the radio source of 3×10^6 years (see Sec. 4.2).

3C 268.4

3C 268.4 is detected at 850µm (5.1±1.2 mJy) but not at 450µm. Recent detections at 170µm and 90µm with ISO and at 1.3 mm with IRAM (6.1 ± 1.6 mJy) indicate a high far-IR luminosity and some synchrotron contamination of the mm fluxes (Andreani et al. 2001). Estimating the millimetre contamination by synchrotron emission is not a trivial matter due to the lack of other data at frequencies higher than 15 GHz (Fig. 1). For reasons to be discussed in Sec. 3 we expect the extended radio lobe spectrum to steepen sharply at high frequencies and the main synchrotron component in the millimetre regime to be the compact core. It is also clear in Fig. 1 that the core spectrum also steepens between 15 GHz and 1.3 mm. To estimate the synchrotron contamination to the 850µm flux-density we assume a millimetre core spectrum with $\alpha = 1$ which gives $S_{850} = 3$ mJy. As we will show below, the properties of the dust spectrum require a contribution to the 850µm flux-density from dust which is in approximate agreement with this contribution from the core.

We have fitted the far-IR and sub-mm data with a range of thermal dust spectra. Using only the ISO fluxes and the 450µm upper limit, the strongly peaked spectrum at $\approx$ 170µm (observed frame) provides strong constraints on the dust temperature and emissivity index (Fig. 1). The best fitting values are $T = 48$ K and $\beta = 2.5$ for dust which is optically-thin at $\lambda > 50\mu$m and this spectrum gives an expected 850µm flux-density of 2.7 mJy. The far-IR luminosity of this dust spectrum is $2 \times 10^{13} \mathrm{L}_\odot$. This value for the emissivity index is larger than usually observed (Priddey & McMahon 2001; Dunne et al. 2000) but requiring β to be no larger than 2.0 gives a similar far-IR luminosity and a higher expected 850µm flux-density of 4.0 mJy. Therefore we conclude that the dust contribution to the 850µm flux-density is significant and independent of its actual value, $L_{\rm FIR} > 2 \times 10^{13} \mathrm{L}_\odot$ and the object is classified as hyperluminous. 3C 268.4 is not heavily reddened in the rest-frame UV but does show strong C IV associated absorption (equivalent width > 1.9 Å; Anderson et al. 1987).

3C 298

The source with the highest 850 µm flux-density in our sample is 3C 298. This quasar is extremely bright at all wavelengths from the radio through to X-rays. It was detected by IRAS at 60 µm and by ISO at five wavelengths ranging from 12.8 to 170 µm (Meisenheimer et al. 2001). 3C 298 has a strong radio core (515 mJy at 5 GHz; Akujor et al. 1991) but is lobe-dominated at GHz frequencies. The measured 1.3 mm flux-density of 14.1 mJy (Meisenheimer et al. 2001) shows that the core is still strong at millimetre wavelengths and makes a substantial contribution to the observed 850 μm flux-density. We have fitted the SED of 3C 298 to attempt to determine the relative contributions of dust and synchrotron emission (Figure 2). This procedure is not trivial because the core spectrum appears to be fairly flat up to a rest-frame frequency of 200 GHz and then steepens sharply to $\alpha \approx 2$ at higher frequencies. However, the flux-density measurements at these high frequencies have large errors and are only 1σ from being consistent with $\alpha = 1$, as is more common above the break in the core spectra of lobe-dominated quasars (e.g. Antonucci, Barvainis & Alloin 1990; van Bemmel & Bertoldi 2001). Therefore we assume a core with $\alpha = 1$ over the observed 1300 to 850 μm range. We conclude that ≈ 8 mJy of the 850 μm flux-density is due to synchrotron radiation and ≈ 13 mJy is due to thermal dust emission. The reason why this quasar was not detected at 450 μm was due to the poor sensitivity caused by the high airmass of the observation. The submillimetre and far-infrared data can be equally well fit by thermal spectra with temperatures $T = 50$ K (typical of starbursts) and $T = 100$ K. The total IR luminosity of 3C 298 is $8 \times 10^{13}\mathrm{L}_{\odot}$.

3C 298 is a small radio source with projected linear size of 12.7 kpc. It shows very strong CIV associated absorption with equivalent width 4.5 Å (Anderson et al. 1987). The optical spectral slope is $\alpha_{\rm opt} = 1.5$, which is redder than typical quasars. This reddening is most likely due to dust associated with the absorbing gas.

3C 318

In Willott, Rawlings & Jarvis (2000b) we have already studied the spectral energy distribution (SED) of 3C 318 and determined a total IR luminosity of $> 7 \times 10^{13}\mathrm{L}_{\odot}$ (corrected for the cosmology used in this paper). The quasar optical spectrum is found to be reddened, indicating the presence of dust in the quasar environment. 3C 318 is a small (6.8 kpc) radio source.

6C 1045+3513

6C 1045+3513 is detected at both 850 and 450 μm, with a submillimetre spectral index of -1.3 ± 0.7. On the basis of the 850 μm observations we find $L_{\rm FIR} > 2 \times 10^{13} L_{\odot}$. In the Appendix we present new optical spectroscopy of this object, showing it to be a reddened quasar, similar to 3C 318. The spectrum also shows a CIV broad absorption feature. 6C 1045+3513 is the smallest radio source of the entire sample of quasars and radio galaxies with a projected linear size of just 1.7 kpc.

2.2 Comparison of radio quasars and radio galaxies

Fig. 3 plots the observed 850 μm flux-density S_{850} against low-frequency (151 MHz) radio luminosity L_{151} for the matched quasar and radio galaxy samples. The main point to note from Fig. 3 is that there is a clear difference in the flux-density distributions of the quasar and radio galaxy samples, with the mean quasar submillimetre flux brighter by a factor of 5.[2]

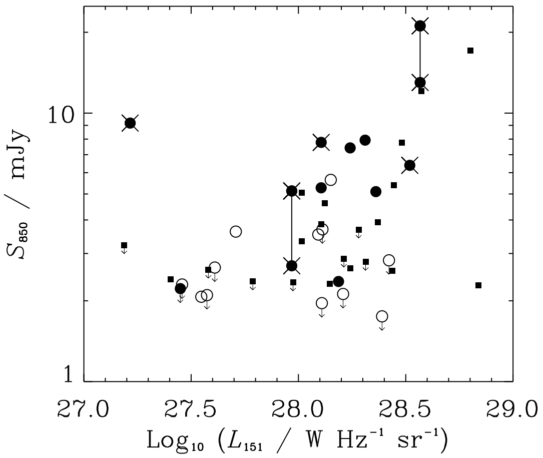

Figure 3. 850 μm flux-density S_{850} against low-frequency (151 MHz) radio luminosity L_{151} for the $1.37 < z < 2.0$ radio quasars (filled circles) and radio galaxies (open circles). 2σ upper limits are denoted by symbols with arrows. The five quasars with detections at shorter wavelengths ($100 - 450$μm) have crosses through them. 3C 298 and 3C 268.4 are shown as two symbols joined by a line, indicating the total flux-density and that corrected for non-thermal emission. Also plotted are radio galaxies at higher redshifts ($2 < z < 4.5$) from A01 (small squares).

Due to the large number of 850 μm upper limits for the radio galaxies, we use survival analysis statistical tests which can account for these limits (Feigelson & Nelson 1985; Isobe, Feigelson & Nelson 1986). Using a variety of tests to compare the 850 μm flux distributions of the quasars and radio galaxies (the Gehan, logrank and Peto-Prentice tests), the flux-density distributions are found to be different at > 99.9% significance. Given the high fraction of upper limits for the radio galaxies, we cannot unequivocally determine the factor by which the quasars are brighter than the radio galaxies in the submillimetre. Using the above tests we find that the quasars are brighter than the radio galaxies by a factor ⩾ 2 at the 95% confidence level.

3 THE SYNCHROTRON CONTRIBUTION TO SUBMILLIMETRE FLUXES

We have found the robust result that radio quasars have $2 - 5$-times higher submillimetre fluxes than radio galaxies of the same radio luminosity and redshift. If this emission is due to optically-thin dust, then this is inconsistent with the notion of radio quasars and radio galaxies being identical apart from some orientation dependence. Given that the radio sources we are discussing are some of the most powerful known, it is essential that we consider whether the observed submillimetre fluxes could be affected by an extrapolation of the nonthermal radio synchrotron emission. Radio lobes and hotspots generally have a very steep spectrum at millimetre wavelengths and are unlikely to contribute significantly for many sources. This issue is discussed in detail in A01 where they find that extended synchrotron components very rarely contribute more than 1 mJy to the 850 µm flux-density. However, A01 note that it is possible that two of the radio galaxy detections in our sample (3C 470 and 6C 0820+3642) become non-detections after correcting for synchrotron emission. We do not attempt to make any corrections for this in this paper, due to the large uncertainties involved in extrapolating the spectrum from radio frequencies. In Sec. 4.2 we will discuss this in terms of the angular extent of the radio sources with respect to the size of the SCUBA beam. Of course, radio quasars and radio galaxies would suffer equally from lobe or hotspot emission, so it cannot explain the difference in submillimetre properties between the two types of object.

---

[2] A second point to note from Fig. 3 is that there is only marginal evidence for a correlation between L_{151} and S_{850}. The survival analysis probability for a correlation being present is ≈ 80%. Removing the outlying point of 6C 1045+3513 increases the correlation probability to ≈ 95%. This matter has been discussed by Archibald et al. (2001), and we defer any further discussion to a wider investigation of the dependences of submillimetre luminosity on radio luminosity and redshift which will use new SCUBA data on radio sources from fainter samples than the 3CR and 6CE samples used here (Rawlings et al., in prep.).

The emission from radio cores and jets is beamed and Doppler boosting makes it highly orientation dependent. In the standard unification scheme, radio quasars have their jet axes closer to our line-of-sight and the enhanced Doppler boosting means that quasars have brighter cores than radio galaxies. Note that because the 3C and 6C radio samples were selected at low frequencies, where extended emission dominates, the quasars in our sample are lobe-dominated and not like the core-dominated blazars which are known to have fairly flat ($0 \leqslant \alpha \leqslant 0.7$) spectra extending into the submillimetre regime (e.g. Gear et al. 1994). There have been few investigations of the radio–millimetre spectral indices of lobe-dominated quasar cores. This is due largely to the fact that their 5 GHz flux-densities are typically in the range $10 - 100$ mJy and, given that their core spectra are not flat, most have been below the sensitivity limit of many millimetre and submillimetre telescopes. In a study of six lobe-dominated quasars, Antonucci, Barvainis & Alloin (1990) find that the typical spectral index between 22 GHz and 230 GHz is $\alpha \approx 1.0$. Van Bemmel & Bertoldi (2001) found the 5–250 GHz spectral indices of three radio quasars to all be ≈ 1. Athreya et al. (1997) compare radio galaxy, lobe-dominated and core-dominated quasar cores and predict that most lobe-dominated quasar cores are flat $\alpha \approx 0$ at GHz frequencies, but steepen at ~ 30 GHz (rest-frame). In Sec. 2 we showed that the core spectra of 3C 268.4 and 3C 298 are also likely to have $\alpha \approx 1$. Another one of our quasar sample, 3C 280.1, has an IRAM 1.25mm flux-density of 3.5 ± 1.7 (Andreani et al. 2001). This suggests its core spectral index from 5 GHz to 1.25 mm is $\alpha \approx 0.7$, again indicating that the 850µm emission must contain a significant contribution from dust. The one example of a flat ($\alpha \approx 0.3$) millimetre spectral index for a lobe-dominated radio source is the unusual radio galaxy 6C 0902+34 (as discussed by A01). The radio properties of this object suggest its jet axis is at a small angle to our line-of-sight and dust obscuration prevents us from observing the nuclear source and classifying it as a quasar (Carilli 1995). Therefore, the available evidence suggests that the core millimetre spectral indices of (lobe-dominated) radio quasars are mostly steep (≈ 1), but with a significant scatter such that some sources will have flatter core spectra.

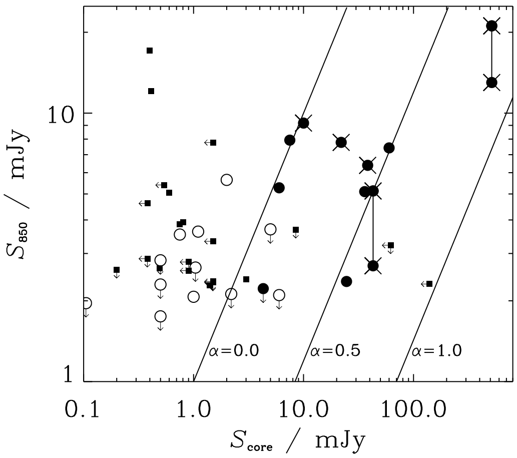

Figure 4. 850 µm flux-density S_{850} against radio core flux-density at 5 GHz $S_{\rm core}$ for radio quasars and radio galaxies (symbols as in Fig. 2). The curves correspond to the predicted contribution of core synchrotron radiation to S_{850} as a function of $S_{\rm core}$ and core spectral index α.

In Fig. 4 we plot S_{850} against the radio core flux-densities at 5 GHz given in Table 1. As expected, the radio quasars have cores which are brighter than those of the radio galaxies by a factor ~ 10. In Fig. 4 we also plot lines corresponding to the expected sub-mm flux-density of the core as a function of core flux-density for a range of spectral indices between 5 GHz and 850 µm. 3C 298 has a core flux a factor of ten greater than any of the other quasars in our study. As we saw in the previous section, its core almost certainly makes a significant contribution to its 850 µm flux of ≈ 10 mJy. If the five quasars on the $\alpha = 0.5$ line all have spectra with $\alpha \approx 1$ then the synchrotron contribution to their 850 µm fluxes is ~ 1 mJy, well below their detected fluxes with the exception of 3C 205. Flatter spectral indices of $\alpha \approx 0.5$ would be necessary for the cores to be responsible for the detections of all these quasars. In reality, it is likely that there is a spread in the GHz to millimetre spectral indices of the quasar cores such that a few of these quasar submillimetre detections might well be influenced by synchrotron emission.

Five of the radio quasars (3C 191, 3C 268.4, 3C 298, 3C 318 and 6C 1045+3513) are detected at shorter far-infrared wavelengths and from their SEDs we are confident that they are dusty hyperluminous objects (Sec. 2). For the other quasars, none of the 450 µm non-detections are sensitive enough for us to be able to exclude the presence of a thermal dust spectrum being responsible for the observed 850 µm emission. 3C 181 and 3C 432 have very weak cores, which are steep ($\alpha > 0.5$) at GHz frequencies and therefore their cores cannot be significant at 850 µm, so we consider these as further secure detections of dust. The IRAM 1.25mm flux of 3C 280.1 suggests that its core component cannot account for all the observed 850 µm flux. The remaining two submillimetre bright quasars (3C 205 and 3C 270.1) lie close to the $\alpha = 0.5$ line in Fig. 4 and we cannot yet be certain that we have detected dust in these objects. Given the available evidence of the likely range of core spectra, we suspect that one or two of these submillimetre detections will be dominated by synchrotron emission. Sensitive millimetre observations of these sources are needed to differentiate between synchrotron and dust. We thus repeated the statistical tests performed in Section 2, now assuming, conservatively, that the submillimetre detections of both of these quasars are due solely to synchrotron emission: the detections were replaced with non-detections of 0.0 ± 1.0 mJy. The mean quasar S_{850} is now 5.2 ± 1.3, still a factor of 4 greater than the mean radio galaxy S_{850} of 1.2 ± 0.6 The survival analysis tests confirm that a statistical difference between the submillimetre fluxes of radio galaxies and quasars remains at 95% significance.

4 WHY DO SOME RADIO QUASARS HAVE HIGH SUBMILLIMETRE LUMINOSITIES?

We have shown that core synchrotron emission may make a small contribution to the 850μm fluxes of 3C radio quasars, but cannot explain all the submillimetre difference between quasars and radio galaxies. In Fig. 3 we showed that there is no systematic difference in the radio luminosities of the two types of object. In this section we consider whether there are any other differences between radio galaxies and quasars which may help to explain the difference in their submillimetre luminosities. The key to following our arguments is that we feel that in any realistic unified scheme we must go beyond the simplest model in which the probability of viewing a quasar nucleus is unity for a viewing angle $\theta \leqslant \theta_{\mathrm{trans}}$, with θ_{trans} constant, and zero at $\theta > \theta_{\mathrm{trans}}$.

4.1 The effect of the intrinsic luminosity of the quasar

As discussed in Sec. 1 the idea that radio galaxies and radio quasars with similar low-frequency radio luminosities should have similar distributions in a second orientation-independent quantity is not quite true. For example, Simpson (1998) has quantified the factor by which quasars should have higher [O III] line strengths than radio galaxies, matched in radio luminosity, in the context of the receding-torus model for AGN (Lawrence 1991). Considering a population of quasars with a spread in optical luminosity, those quasars with higher optical luminosities have a larger torus opening angle due to the radius at which dust is sublimated being larger. Taking into account the scatter in the correlation between radio and optical luminosity, this means that sources with higher optical luminosities can be viewed within a larger opening angle and are thus more likely to be classified as quasars. An additional effect is that the larger opening angles allow a greater fraction of the ionizing continuum to escape, however this is not the dominant effect in this case. Simpson (1998) showed that this leads to a sample of radio quasars having a mean optical luminosity, as probed by their [O III] line luminosity, approximately twice that of a sample of radio galaxies of the same radio luminosity.

In Fig. 5 we plot S_{850} against the [O III] emission line luminosity $L_{[\mathrm{O\,III}]}$, which is emitted isotropically, believed to be produced outside any obscuring torus, and which is a good indicator of the ionizing luminosity (Simpson 1998). Correlation tests show that S_{850} and $L_{[\mathrm{O\,III}]}$ for the radio quasars and radio galaxies are positively correlated at 95% significance. It is also apparent that the quasars do typically have higher $L_{[\mathrm{O\,III}]}$ than the radio galaxies. For the quasars the mean $\log(L_{[\mathrm{O\,III}]}/\mathrm{W})$ is 36.9 ± 0.1 and for the radio galaxies it is 36.2 ± 0.2. Thus there is a factor of five difference in the mean [O III] luminosities of the two types of object in our sample. A similar difference between $L_{[\mathrm{O\,III}]}$ for the highest radio luminosity quasars and radio galaxies is also evident from Fig. 5 of Jackson & Rawlings (1997). In that study, all the objects have [O III] line observations made with the same wide slit, thereby eliminating uncertainties due to inhomogeneous datasets. This difference in emission line luminosity (and consequently ionizing luminosity) could explain the difference of a factor a few in the average luminosities of quasars and radio galaxies in the mid- and far-infrared in studies with IRAS and ISO (Heckman et al. 1994; Hes et al. 1995; van Bemmel, Barthel & de Graauw 2000; Meisenheimer et al. 2001), since this radiation is certainly dominated by nuclear emission reprocessed by the dust torus.

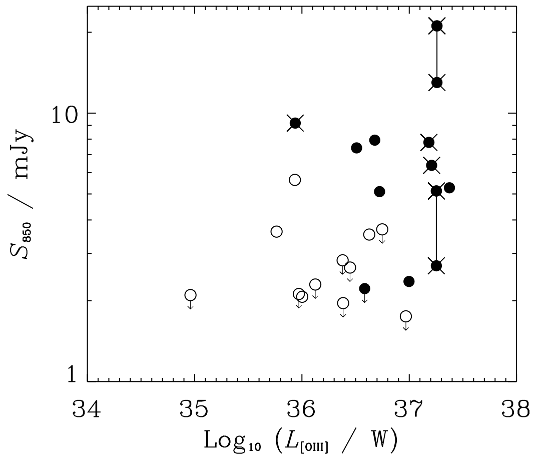

Figure 5. 850 μm flux-density S_{850} against narrow [O III] emission line luminosity $L_{[\mathrm{O\,III}]}$ for radio quasars and radio galaxies (symbols as in Fig. 2).

Could such an effect also be responsible for the similar factor difference in the submillimetre luminosities of radio quasars and radio galaxies? This would require a tight correlation between the submillimetre and optical continuum emission from quasars. The analysis of Simpson (1998), predicting a factor of two difference in the [O III] luminosities of radio quasars and radio galaxies, used the known scatter of 0.6 dex in the radio–optical correlation (Serjeant et al. 1998; Willott 2000). Therefore, we would expect the scatter exhibited in the radio–submillimetre correlation to be of the same order if the submillimetre and optical continua are tightly correlated. A power law fit to the marginal correlation between L_{151} and S_{850} in Fig.2 gives a linear slope with a scatter of 0.3 dex. The scatter may be slightly larger than this because of the large number (40%) of non-detections (in the above analysis non-detections were set to their 1σ upper limits). However, within the limited range in L_{151} available in our study, we find the scatter in the radio–submillimetre correlation to be no larger than that of the radio–optical correlation.

A tight correlation between submillimetre and optical luminosities could probably only come about by direct heating of the dust responsible for the submillimetre emission by the AGN (as is known to be the case for the mid-infrared emission, and has been discussed previously by Willott et al. 2000b). In this case the scatter could be as small as that seen in the correlation between optical and mid-infrared luminosities of optically-bright, low-redshift quasars, i.e. 0.2 dex from the study of Rowan-Robinson (1995). If the far-infrared emission is due to dust heated by an intense starburst rather than by the quasar, a larger scatter is predicted; indeed the larger scatter, of 0.4 dex, in the far-infrared versus optical luminosity plot from Rowan-Robinson (1995) was used as an argument that: (i) the far-infrared emission from the low-redshift quasars is dominated by starburst-heated dust; and (ii) the scaling relation between optical and far-infrared luminosities arises from both quantities being correlated with a third variable, i.e. the black hole and/or galaxy mass. However, in the quasar-heating hypothesis, the far-infrared luminosity is strongly dependent upon the extended dust distribution (e.g. Granato & Danese 1994) and would indeed be expected to show a larger scatter than the mid-infrared–optical ratio. It may seem surprising that objects with such large quantities of dust have such a small scatter in these ratios because of the effects of dust-reddening of the optical emission. However, in both the Rowan-Robinson sample and the radio-loud sample discussed in this paper, objects would not be classified as quasars if they were heavily reddened ($A_V \gtrsim 3$).

Finally in this section, we note that despite the quantitative agreement between the predictions of the receding-torus model and the submillimetre difference between radio quasars and radio galaxies, other physical effects seem likely to be important. Note, for example, that the high submillimetre luminosity of 6C 1045+3513 is an anomaly in the receding-torus model, since it has a value of $L_{[\mathrm{O\,III}]}$ below that of all the 3C radio galaxies.

4.2 The effect of the radio source age

Fig. 6 plots S_{850} against the projected linear sizes D of the radio sources. According to unified schemes, quasars will typically have projected linear sizes a factor of ≈ 1.6 smaller than those of radio galaxies, due to the smaller angles between their jet axes and our line-of-sight. (assuming $\theta_{\rm trans} = 53^\circ$ from Willott et al. 2000a). Taking account of this effect, the distributions in D for the quasars and radio galaxies are fairly similar. However, a striking feature of this plot is that the quasars appear to show an anti-correlation between S_{850} and D. The correlation tests performed (Kendal's Tau and Cox's) show these quantities to be anti-correlated with significances of 95 and 99%, respectively. Including the radio galaxies as well, and accounting for projection effects, the significance of this correlation is only marginal (92% and 50%), largely because of the introduction of a large number of submillimetre upper limits.

An important point to consider here is whether this anti-correlation could be due to contamination of the sub-millimetre emission by synchrotron from the lobes or hotspots. This is because the SCUBA beam at 850 μm has a 13 arcsec FWHM, corresponding to a physical size at these redshifts of 110 kpc. Hence sources with D less than this value will have their hotspots within the SCUBA beam. However, one should note that the five radio quasars with detections at shorter wavelengths indicated by the crosses are also mostly the smallest quasars. In these objects we have evidence for a thermal dust spectrum and high far-IR luminosities. It can also be seen that five radio galaxies have $D < 100$ kpc and these have significantly smaller submillimetre fluxes than the quasars. In the orientation-based unified scheme there is no reason why quasars should have brighter extended synchrotron emission than radio galaxies. Therefore, although we cannot rule out some lobe/hotspot contamination in the smallest sources it cannot be the driving force behind the observed correlation.

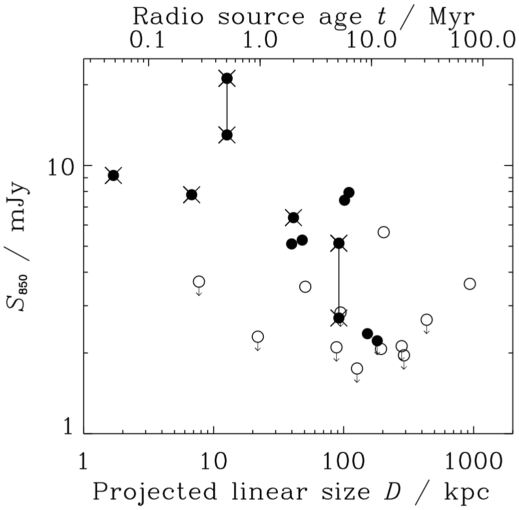

Figure 6. 850 μm flux-density S_{850} against radio source projected linear size D for radio quasars and radio galaxies (symbols as in Fig. 2). There is a significant anti-correlation present for the quasars. The upper axis shows how the ages of radio sources approximately relate to D, according to the model of Willott et al. (1999) (see Sec. 4.2 for details).

3C 298, 3C 318, 6C 1045+3513, and more marginally 3C 191, are all compact steep-spectrum (CSS) radio sources, which are believed to be small due to their jets being triggered relatively recently ($\sim 10^6$ years; Fanti et al. 1995). Previous studies of the far-infrared properties of CSS sources have shown them to be indistinguishable from larger, presumably older, radio sources (Heckman et al. 1994; Fanti et al. 2000). However our study is quite different from these which were limited to low redshifts (and hence luminosities) due to the sensitivity limitations of IRAS and ISO, and it is plausible that the differences only occur at higher luminosities, higher redshifts and/or longer wavelengths (e.g. because the emission is dominated by starburst-heated cold-dust emission rather than AGN-heated hot-dust torus emission).

It is also interesting to note that 3C 298, 3C 318 and 6C 1045+3513 are reddened quasars, indicating significant quantities of dust in their host galaxies. Also, 3C 191, 3C 268.4 and 3C 298, show very strong CIV associated absorption and 6C 1045+3513 has a CIV broad absorption system. Baker et al. (2001) show that there is an anti-correlation between the strength of associated absorption systems and radio linear size and also that the redder quasars tend to have the strongest line absorption. It has also been noticed that, amongst radio-loud quasars, broad absorption lines are more commonly observed in the smallest radio sources (Becker et al. 2000). These observations indicate an evolutionary picture where the absorbing material is cleared as the radio sources get older (Baker et al. 2001). This is similar to the evolutionary scheme of Sanders et al. (1988) where quasars begin their lives in a dust-enshrouded phase.

The projected linear size D of a radio quasar or radio galaxy can be related approximately to the time since the jets were triggered t, since the relationship between these variables is only weakly dependent upon the radio luminosity, and the objects under consideration span only 1.5 dex in this quantity. Using the simple model of radio source evolution in Willott et al. (1999) we can, at least approximately, transform the linear size axis in Fig. 6 to the time since the quasars were triggered (the radio galaxies have ages on average a factor of 1.6 smaller at a given D than shown here, due to projection effects). Fig. 6, and the anti-correlation it exhibits, shows that the most submillimetre-luminous quasars had their radio sources triggered $< 10^7$ years ago. This means that the processes controlling the submillimetre/far-infrared luminosity $L_{\rm FIR}$ are synchronized with the jet-triggering event and that $L_{\rm FIR}$ declines on a $\sim 10^7$ yr timescale.

Although high values of $L_{\rm FIR}$ for an AGN are generally interpreted as evidence for high rates of star formation, it is possible that, as explored in Sec. 4.1 (see also Willott et al. 2000b; Rowan-Robinson 2000), even the cool dust is directly heated by the AGN. Any evidence for star formation is indirect, being based on the large gas masses observed in CO in a handful of cases, but mostly deduced from the large dust masses required by any submillimetre-detected thermal source (e.g. Hughes, Dunlop, & Rawlings 1997). With a standard dusty disc model (e.g. Efstathiou & Rowan-Robinson 1995) there are difficulties in heating the cool dust at large distances from the nucleus, due to the fact the disc is optically thick and shields the distant dust from the ionizing radiation. A more efficient way of heating large amounts of cool dust by an AGN, come from models where the dust has a more isotropic distribution with a very high covering factor (e.g. Granato, Danese & Franceschini 1996). This may occur preferentially in recently-triggered AGN if the dusty gas fueling the nucleus is not in a regular torus distribution. In addition, models for shocks caused by advancing radio components suggest that dust grains cannot survive for much longer than $\sim 10^7$yr in such environments (De Young 1998). Jarvis et al. (2001b) summarise other evidence that expanding radio sources modify the physical conditions of their gaseous environments as the radio-emitting components expand outward after jet triggering. There are therefore two reasons why in a scenario in which quasar-heated dust dominates, one expects $L_{\rm FIR}$ to decline on a $\sim 10^7$yr timescale. Note that the fact that the brightest submillimetre sources are reddened quasars with line absorption is consistent with this picture, since with this dust distribution there is a high probability of our line-of-sight to the nucleus intercepting a dust cloud. It is of course possible that the dust distribution could be influenced by previous episodes of star-formation.

It is also possible that the submillimetre emission in the hyperluminous sources is dominated by starburst-heated dust, in which case the implication is that the jet-triggering process is accurately synchronized with an intense burst of star formation. The timescale for such star formation events would have to be $\lesssim 10^7$ years for the far-infrared (300 μm) luminosity to peak $\approx 10^7$ yr after the onset of the starburst (Efstathiou, Rowan-Robinson & Siebenmorgen 2000). Line ratios from mid-infrared spectroscopy of nearby starburst galaxies suggest that the duration of the bursts in such galaxies are $\sim 10^7$ yr (Thornley et al. 2000) and for ultraluminous infrared galaxies $\sim 2 \times 10^7$ yr (Genzel et al. 1998). Thus the starburst timescales are quite consistent with the hypothesis that a starburst and a jet-producing AGN were triggered synchronously, and the anti-correlation seen in Fig. 6.

A starburst of such a brief duration, forming stars at ~ 1000 M$_\odot$ yr^{-1} as implied by the submillimetre luminosity, would form $\sim 10^{10}$ M$_\odot$ of stars over its lifetime. The total stellar mass of a powerful radio galaxy with a luminosity of 5L$_\star$ (Jarvis et al. 2001a) is 5×10^{11}M$_\odot$. Therefore such a star formation episode would form only a few per cent of the total stellar mass in a massive elliptical galaxy and therefore this phase is not a major event in the star-formation histories of the quasar host galaxy. This is consistent with other evidence, such as the small scatter in the $K - z$ relation (Jarvis et al. 2001a) and the existence of very red radio galaxies at $1 < z < 2$ (Dunlop et al. 1996; Dunlop 1999; Willott, Rawlings & Blundell 2001), that the bulk of the stars in powerful radio galaxies were formed at higher redshifts of $z > 3$.

Regardless of whether the dust is heated by a quasar or a starburst or a mixture of the two, it seems that Fig. 6 provides some support for the Blundell & Rawlings (1999) conjecture that radio source youth may be an important factor in explaining the high submillimetre luminosities of distant radio galaxies. An important question is how this finding relates to the properties of the more distant ($z > 2$) systems studied by A01. We again defer a more detailed discussion to a future paper (Rawlings et al. in prep.) but note here that the fact that the submillimetre luminosities of the $z < 2$ radio quasars are similar to the radio galaxies at $z > 2$ is not, by itself, a strong argument that their host galaxies are in similar evolutionary states. It is certainly plausible that the higher-redshift objects are forming significant fractions of the stellar mass of a giant elliptical galaxy, requiring simply that the duration of the starburst is $\gg 10^7$ yr. Direct measurements of gas mass, e.g. by CO observations, would be very important for determining the evolutionary states and the main heating source of the cool dust for the $z \sim 1.5$ objects studied here. It is hard with submillimetre continuum measurements alone to determine the relationship between these objects and the high-redshift radio galaxies studied by A01. The discovery of huge reservoirs of molecular gas in some very high-redshift radio galaxies (Papadopoulos et al. 2000; Alloin, Barvainis & Guilloteau 2000) supports a starburst-heating model for the bulk of the submillimetre continuum in these objects, and the lack of such reservoirs at $z \sim 1.5$, if observed, would suggest that quasar-heating might become more prevalent at lower redshifts.

5 CONCLUDING REMARKS

We have performed a submillimetre survey of radio quasars in the redshift range $1.37 < z < 2$ and detect ten out of eleven quasars, implying submillimetre/far-infrared luminosities $\gtrsim 4 \times 10^{12}\mathrm{L}_{\odot}$. We argue that only one or two of these detections are dominated by core synchrotron emission. For five quasars, detections at shorter wavelengths confirm the presence of a thermal continuum and a large mass ($\sim 10^{8}\mathrm{M}_{\odot}$) of cool dust.

We find the radio quasars have higher submillimetre luminosities by a factor of ~ 5 than radio galaxies of the same radio luminosity and redshift, a factor which cannot be reduced below ~ 2 by accounting for possible synchrotron contamination. At $z \sim 1.5$ radio quasars are intrinsically brighter than radio galaxies at submillimetre wavelengths. This argues against the simplest unified scheme for radio sources in which the probability of viewing a quasar nucleus is unity for a viewing angle $\theta \leqslant \theta_{\mathrm{trans}}$, with θ_{trans} constant, and zero at $\theta > \theta_{\mathrm{trans}}$. It is, however, in quantitative agreement with a receding-torus model in which θ_{trans} depends on quasar optical luminosity, but only if there is a close relationship between optical luminosity and L_{FIR}. The implication is that quasar-heated dust dominates L_{FIR} for powerful radio quasars at $z \sim 1.5$.

There is a significant anti-correlation between L_{FIR} and radio source age in the sense that hyperluminous quasars tend to be associated with young ($< 10^{7}$ yr) sources at $z \sim 1.5$. This means that the processes controlling L_{FIR} are synchronized with the jet-triggering event and that L_{FIR} declines on a $\sim 10^{7}$ yr timescale. There is evidence for a small amount of obscuration in the most submillimetre-luminous quasars from reddening (3C 298, 3C 318 and 6C 1045+3513) and/or prominent associated absorption (3C 191, 3C 268.4, 3C 298) or broad absorption lines (6C 1045+3513). We speculate that shortly after jet triggering, dust is more widely distributed than at later times. This distributed dust could be heated by the quasar nucleus and/or a short-lived synchronized starburst and may be destroyed by shocks associated with the expanding radio source. Any such starburst would form only a few per cent of the total stellar mass in agreement with the evidence for dominant old stellar populations in $z \sim 1.5$ radio galaxies.

ACKNOWLEDGEMENTS

We thank the anonymous referee for some very useful suggestions. We are very grateful to the staff at the Joint Astronomy Centre for their help with the observations. The JCMT is operated by the Joint Astronomy Centre on behalf of the U.K. Particle Physics and Astronomy Research Council. The William Herschel Telescope is operated on the island of La Palma by the Isaac Newton Group in the Spanish Observatorio del Roque de los Muchachos of the Instituto de Astrofisica de Canarias. This research has made use of the NASA/IPAC Extra-galactic Database, which is operated by the Jet Propulsion Laboratory, Caltech, under contract with the National Aeronautics and Space Administration. CJW thanks PPARC for support.

REFERENCES

Akujor C.E., Spencer R.E., Zhang F.J., Davis R.J., Browne I.W.A., Fanti C., 1991, MNRAS, 250, 215
Alloin D., Barvainis R., Guilloteau S., 2000, ApJ, 528L, 81
Anderson S.F., Weymann R.J., Foltz C.B., Chaffee F.H., 1987, AJ, 94, 278
Andreani P., Fosbury R.A.E., van Bemmel I., Freudling W., 2001, A&A, in press, astro-ph/0111064
Antonucci R.R.J., 1993, ARA&A, 31, 473
Antonucci R.R.J., Barvainis R., Alloin D., 1990, ApJ, 353, 416
Archibald E.N., Dunlop J.S., Hughes D.H., Rawlings S., Eales S.A., Ivison R.J., 2001, MNRAS, 323, 417 (A01)
Athreya R.M., Kapahi V.K., McCarthy P.J., van Breugel W., 1997, MNRAS 289, 525
Baker J.C., Hunstead R.W., Athreya R.M., Barthel P.D., De Silva E., Lehnert M.D., Saunders R.D.E., 2001, ApJ, submitted
Barthel P.D., 1989, ApJ, 336, 606
Barthel P.D., Tytler D.R., Thomson B., 1990, A&AS, 82, 339
Becker R.H., White R.L., Gregg M.D., Brotherton M.S., Laurent-Muehleisen S.A., Arav N., 2000, ApJ, 538, 72
Bettoni D., Falomo R., Fasano G., Govoni F., Salvo M., Scarpa R., 2001, A&A, 380, 471
Blain A.W., Longair M.S., 1993, MNRAS, 264, 509
Blundell K.M., Rawlings S., 1999, Nature, 339, 330
Brotherton M.S., Tran H.D., Becker R.H., Gregg M.D., Laurent-Muehleisen S.A., White R.L., 2001, ApJ, 546, 775
Carilli C.L., 1995, A&A, 298, 77
De Young D.S., 1998, ApJ, 507, 161
Dunlop J.S., 1999, in The Most Distant Radio Galaxies, ed. P.N. Best, H.J.A. Röttgering, M.D. Lehnert, (KNAW Colloq.; Dordrecht: Kluwer), 14
Dunlop J.S., Peacock J.A., Spinrad H., Dey A., Jimenez R., Stern D., Windhorst R., 1996, Nature, 381, 581
Dunlop J.S., McLure R.J., Kukula M.J., Baum S.A., O'Dea C.P., Hughes D.H., 2001, MNRAS, submitted, astro-ph/0108397
Dunne L., Eales S.A., Edmunds M., Ivison R., Alexander P., Clements D.L., 2000, MNRAS, 315, 115
Efstathiou A., Rowan-Robinson M., 1995, MNRAS, 273, 649
Efstathiou A., Rowan-Robinson M., Siebenmorgen R., 2000, MNRAS, 313, 734
Espey B.R., Carswell R.F., Bailey J.A., Smith M.G., Ward M.J., 1989, ApJ, 342, 666
Fanti C., Fanti R., Dallacasa D., Schilizzi R.T., Spencer R.E., Stanghellini C., 1995, A&A, 302, 317
Fanti C., et al., 2000, A&A, 358, 499
Feigelson E.D., Nelson P.I., 1985, ApJ, 293, 192
Gear W.K., et al., 1994, MNRAS, 267, 167
Genzel R., et al., 1998, ApJ, 498, 579
Granato G.L., Danese L., 1994, MNRAS, 268, 235
Granato G.L., Danese L., Franceschini A., 1996, ApJL, 460, 11
Gregg M.D., Becker R.H., Brotherton M.S., Laurent-Meuleisen S.A., Lacy M., White R.L., 2000, ApJ, 544, 142
Hamann F.W., Barlow T.A., Chaffee F.C., Foltz C.B., Weymann R.J., 2001, ApJ, 550, 142
Heckman T.M., O'Dea C.P., Baum S.A., Laurikainen E., 1994, ApJ, 428, 65
Hes R., Barthel P.D., Hoekstra H., 1995, A&A, 303, 8
Hirst P., Jackson N., Rawlings S., 2002, MNRAS, submitted
Hughes D.H., Dunlop J.S., Rawlings S., 1997, MNRAS, 289, 766
Isobe T., Feigelson E.D., Nelson P.I., 1986, ApJ, 306, 490
Jackson N., Rawlings S., 1997, MNRAS, 286, 241
Jarvis M.J., Rawlings S., Eales S.A., Blundell K.M., Bunker A.J., Croft S., McLure R.J., Willott C.J., 2001a, MNRAS, 326, 1585
Jarvis M.J., et al., 2001b, MNRAS, 326, 1563
Laing R.A., Riley J.M., Longair M.S., 1983, MNRAS, 204, 151
Lawrence A., 1991, MNRAS, 252, 586

Magorrian J., et al., 1998, AJ, 115, 2285
McCarthy P.J., 1993, ARA&A, 31, 639
McLure R.J., Kukula M.J., Dunlop J.S., Baum S.A., O'Dea C.P., Hughes D.H., 1999, 308, 377
Meisenheimer K., Haas M., Muller S.A.H., Chini R., Klaas U., Lemke D., 2001, A&A, 372, 719
Miller P., Rawlings S., Saunders R., Eales S.A., 1992, MNRAS, 254, 93
Nolan L.A., Dunlop J.S., Kukula M.J., Hughes D.H., Boroson T., Jimenez R., 2001, MNRAS, 323, 308
Owen F.N., Laing R.A., 1989, MNRAS, 238, 357
Papadopoulos P.P., Röttgering H.J.A., van der Werf P.P., Guilloteau S., Omont A., van Breugel W.J.M., Tilanus R.P.J., 2000, ApJ, 528, 626
Priddey R.S., McMahon R.G., 2001, MNRAS, 324L, 17
Rawlings S., Saunders R., 1991, Nature, 349, 138
Rawlings S., Eales S.A., Lacy M., 2001, MNRAS, 322, 523
Rowan-Robinson M., 1995, MNRAS, 272, 737
Rowan-Robinson M., 2000, MNRAS, 316, 885
Sanders D.B., Soifer B.T., Elias J.H., Madore B.F., Matthews K., Neugebauer G., Scoville N.Z., 1988, ApJ, 325, 74
Scheuer P.A.G., 1987, in *Superluminal Radio Sources*, edited by J.A. Zensus and T.J. Pearson, p.331, Cambridge University Press
Serjeant S., Rawlings S., Maddox S.J., Baker J.C., Clements D., Lacy M., Lilje P.B., 1998, MNRAS, 294, 494
Simpson C., 1998, MNRAS, 297, L39
Spinrad H., Marr J., Aguilar L., Djorgovski S., 1985, PASP, 97, 932
Thornley M.D., Schreiber N.M.F., Lutz D., Genzel R., Spoon H.W.W., Kunze D., Sternberg A., 2000, ApJ, 539, 641
van Bemmel I.M., Bertoldi F., 2001, A&A, 368, 414
van Bemmel I.M., Barthel P.D., de Graauw T., 2000, A&A, 359, 523
Willott C.J., 2000, to appear in Proc. "AGN in their Cosmic Environment", eds. B. Rocca-Volmerange, H. Sol, EDPS Conf. Series in Astron. & Astrophysics, astro-ph/0007467
Willott C.J., Rawlings S., Blundell K.M., Lacy M., 1998, MNRAS, 300, 625
Willott C.J., Rawlings S., Blundell K.M., Lacy M., 1999, MNRAS, 309, 1017
Willott C.J., Rawlings S., Blundell K.M., Lacy M., 2000a, MNRAS, 316, 449
Willott C.J., Rawlings S., Jarvis M.J., 2000b, MNRAS, 313, 237
Willott C.J., Rawlings S., Blundell K.M., 2001, MNRAS, 324, 1

APPENDIX A: 6C 1045+3513 - A SUBMILLIMETRE-LUMINOUS REDDENED BAL QUASAR

In this appendix we present a new optical spectrum of 6C 1045+3513, which is one of the brightest radio quasars at submillimetre wavelengths found in this paper ($S_{850} = 9.18 \pm 1.10$ mJy). It is also detected at the 3σ level with the short wavelength array ($S_{450} = 21.3 \pm 6.8$ mJy).

6C 1045+3513 was observed with the ISIS double-beam spectrograph on the William Herschel Telescope on April 16 2001. Conditions were photometric with 1.0 arcsec seeing and a 1.0 arcsec slit was used giving a dispersion resolution of 8 Å. The telescope was pointed at the position of the compact radio source (10:48:34.25 +34:57:25.0 - J2000.0). The total integration time of the observation was 1200 seconds. The data were reduced in the IRAF package using the same method as in Willott et al. (1998). The red and blue arm spectra were joined together, averaging over 35 Å where the signal-to-noise ratio of the spectra were approximately equal (6200 Å).

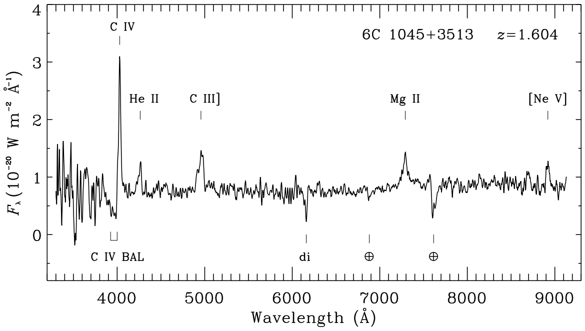

Figure A1. Optical spectrum of the reddened quasar 6C 1045+3513 with emission lines labelled. The CIV broad absorption feature is also marked. The absorption features marked with ⊕ are due to atmospheric absorption and that marked 'di' is an artefact caused by the dichroic.

The target is clearly identified in the two dimensional spectrum and appears to be spatially unresolved. In Figure A1 we show the optical spectrum extracted in a 1 arcsec aperture. The object has a red continuum and several strong emission lines (see Table A1). The red continuum has a spectral index of 2.3 and is well fit by a quasar spectrum reddened by $A_{\rm V} = 1.5$ (assuming a Milky-Way extinction curve). The positions of the emission lines are consistent with a redshift for 6C 1045+3513 of $z = 1.604$, extremely close to the tentative value reported by Rawlings et al. (2001). The C IV and He II emission lines are both narrow (FWHM $\approx$ 2000 km s^{-1}). The Mg II and C III] emission lines appear to have narrow central profiles with broad wings, which together with the weak or absent broad wings in C IV and He II, are consistent with broad-line region reddening of the same amount as the continuum fitting suggests.

There is very high equivalent width C IV absorption on the blue wing of the emission line. This feature is very broad with a width of at least 6000 km s^{-1}. There is no corresponding broad absorption of Mg II, so 6C 1045+3513 is classified as a high-ionization broad absorption line (BAL) quasar. Unfortunately, our data are not sensitive enough or with sufficient spectral resolution to determine the structure of the absorption trough. 6C 1045+3513 is one of the most radio-luminous quasars to show the BAL phenomenon, with a radio luminosity similar to that of the BAL QSO FIRST J101614.3+520916 (Gregg et al. 2000) .

6C 1045+3513 is thus remarkably similar to 3C 318 (Willott et al. 2000b). Both objects have a small degree of reddening which suppresses the rest-frame UV broad line strengths to below those of the narrow lines. Both are also very luminous submillimetre sources (with detections at both 850 µm and 450 µm) and both are compact ($D < 10$ kpc) radio sources with similar estimated source ages. A possible reason for these similarities is discussed in Sec. 4.2.

Line	λ_{obs} (Å)	z_{em}	FWHM (km s^{-1})	Flux/10^{-19} (W m^{-2})
C IV λ1549	4029 ± 4	1.601	2000	18 ± 4
He II λ1640	4263 ± 6	1.599	2400	3.6 ± 1.3
C III] λ1909	4906 ± 6	1.597	4300	8.2 ± 1.0
Mg II λ2799	7291 ± 2	1.605	2900	9 ± 4
[Ne V] λ3426	8920 ± 3	1.604	1300	4.6 ± 1.6

Table A1. Emission line data for 6C 1045+3513 from our optical spectrum. Fluxes have been aperture corrected.